Innate and Adaptive Immune Functions of Peyer's Patch Monocyte-Derived Cells Article Innate and Adaptive Immune Functions of Peyer's Patch Monocyte-Derived Cells

Johnny Bonnardel, Clément da Silva, Sandrine Henri, Samira Tamoutounour, Lionel Chasson, Frederic Montañana-Sanchis, Jean-Pierre Gorvel, Hugues Lelouard

HAL Id: hal-01212685

https://amu.hal.science/hal-01212685

Submitted on 7 Oct 2015

Article

Innate and Adaptive Immune Functions of Peyer's Patch Monocyte-Derived Cells

Graphical Abstract
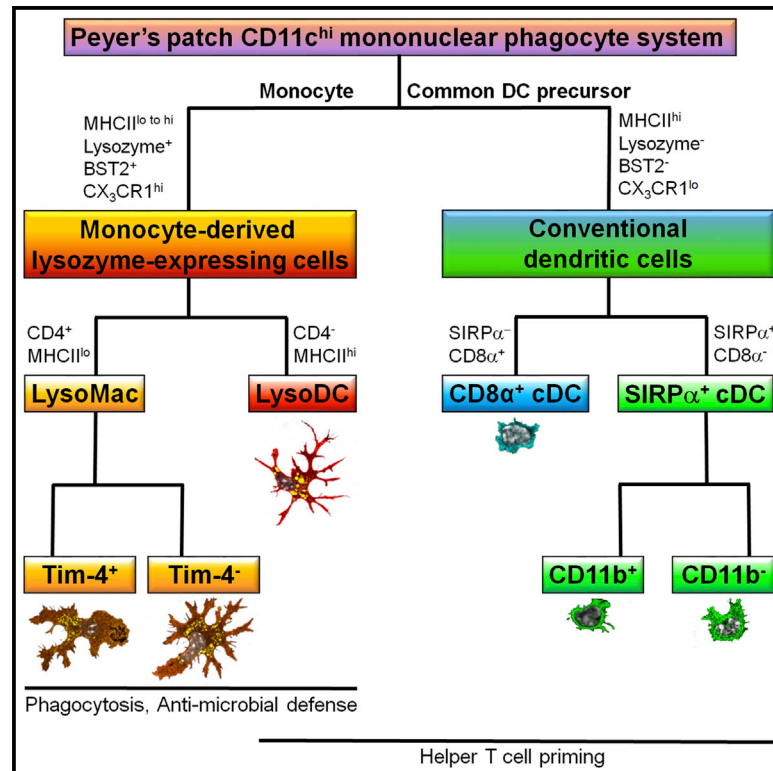
Authors

Johnny Bonnardel, Clément Da Silva, ...,
Jean-Pierre Gorvel, Hugues Lelouard

Correspondence

lelouard@ciml.univ-mrs.fr

In Brief

Bonnardel et al. provide a comprehensive analysis of the phenotype, distribution, ontogeny, lifespan, function, and transcriptional profile of Peyer's patch (PP) mononuclear phagocyte system. They show that, at steady state, monocytes give rise locally to both macrophages and lysozyme-expressing DCs.

Highlights

- Monocytes give rise to macrophages and LysoDCs in Peyer's patches

- LysoDCs and macrophages are the main phagocytic cells of PPs

- PP LysoDCs and macrophages display innate antiviral and antibacterial gene signatures

- Short-lived LysoDCs efficiently prime naive helper T cells toward Th1 cells

Accession Numbers

GSE65514

Article

Innate and Adaptive Immune Functions of Peyer's Patch Monocyte-Derived Cells

Johnny Bonnardel,[1,2,3] Clément Da Silva,[1,2,3] Sandrine Henri,[1,2,3] Samira Tamoutounour,[1,2,3] Lionel Chasson,[1,2,3] Frederic Montañana-Sanchis,[1,2,3] Jean-Pierre Gorvel,[1,2,3] and Hugues Lelouard[1,2,3,*]
[1]Centre d'Immunologie de Marseille-Luminy (CIML), Aix-Marseille University, UM2, 13288 Marseille, France
[2]Institut National de la Santé et de la Recherche Médicale (INSERM), U1104, 13288 Marseille, France
[3]Centre National de la Recherche Scientifique (CNRS), UMR7280, 13288 Marseille, France
*Correspondence: lelouard@ciml.univ-mrs.fr
http://dx.doi.org/10.1016/j.celrep.2015.03.067

SUMMARY

Peyer's patches (PPs) are primary inductive sites of mucosal immunity. Defining PP mononuclear phagocyte system (MPS) is thus crucial to understand the initiation of mucosal immune response. We provide a comprehensive analysis of the phenotype, distribution, ontogeny, lifespan, function, and transcriptional profile of PP MPS. We show that monocytes give rise to macrophages and to lysozyme-expressing dendritic cells (LysoDCs), which are both involved in particulate antigen uptake, display strong innate antiviral and antibacterial gene signatures, and, upon TLR7 stimulation, secrete IL-6 and TNF, but neither IL-10 nor IFNγ. However, unlike macrophages, LysoDCs display a rapid renewal rate, strongly express genes of the MHCII presentation pathway, and prime naive helper T cells for IFNγ production. Our results show that monocytes differentiate locally into LysoDCs and macrophages, which display distinct features from their adjacent villus counterparts.

INTRODUCTION

To protect our body from harmful agents, the mammalian small intestine possesses specific sentinel sites called Peyer's patches (PPs) where mucosal immune response initiation and generation of immunoglobulin A-producing B cells take place (Macpherson et al., 2012). PPs comprise clustered domes formed by B cell follicles separated from each other by interfollicular regions (IFRs) enriched in T cells. The follicle-associated epithelium (FAE) contains specialized epithelial cells, called M cells, that bind and rapidly transport microorganisms from the lumen to the subepithelial dome (SED) (Owen and Jones, 1974; Schulz and Pabst, 2013). There, antigen uptake, degradation, and presentation by cells of the mononuclear phagocyte system (MPS) are crucial steps to induce the mucosal immune response. The MPS comprises monocytes, dendritic cells (DCs), and macrophages. PP DCs encompass five different subsets: plasmacytoid DCs (pDCs), CD8α+ DCs, CD11b+ DCs, double-negative DCs (DN DCs), and lysozyme-expressing DCs (LysoDCs)

(Contractor et al., 2007; Iwasaki and Kelsall, 2001; Lelouard et al., 2010). The pDCs and DN DCs are mainly located in the SED and in the IFR, whereas CD8α+ DCs are situated in the IFR and CD11b+ DCs and LysoDCs in the SED. In addition, DN DCs and LysoDCs can penetrate into the FAE where they interact with M cells (Iwasaki and Kelsall, 2001; Lelouard et al., 2012).

Among PP DCs, LysoDCs are the most efficient at taking up pathogenic bacteria, dead cells, and particulate antigens in vivo (Lelouard et al., 2010, 2012). Moreover, they are able to internalize luminal antigens by extending dendrites into the gut lumen through M cell-specific transcellular pores (Lelouard et al., 2012). Although Salmonella Typhimurium is mainly internalized by LysoDCs, which express the chemokine receptor CX3CR1, the associated immune response seems to be mediated by CCR6+CX3CR1− DCs, which correspond either to DN DCs or CD11b+ DCs (Lelouard et al., 2010; Salazar-Gonzalez et al., 2006; Zhao et al., 2003). DN DCs and CD8α+ DCs produce IL-12 in response to bacterial stimulation, while CD11b+ DCs produce IL-10 and IL-6 and induce IgA secretion in vitro (Iwasaki and Kelsall, 2001; Sato et al., 2003). CD11b+ DCs also are able to prime naive T cells to secrete IL-4 and IL-10 (Iwasaki and Kelsall, 2001). However, since LysoDCs express high levels of CD11b and can't be discriminated from CD11b+ DCs based on commonly used criteria of isolation (e.g., CD11c, MHCII, and CD11b), it is yet unknown whether these functional properties are shared by both of these PP DC subsets. Moreover, it is worth noting that no distinction has been made so far between DCs of the dome and DCs of dome-associated villi (DAVs), which could have been co-isolated and might have distinct properties.

Unlike PP DCs, the phenotype, diversity, immune functions, and distribution of macrophages in PPs are still unknown due to the lack of reliable markers.

Here we used a combination of comparative transcriptional analyses, multiparameter flow cytometry, and high-resolution confocal microscopy to study the diversity, distribution, origin, renewal, and function of the PP MPS. We show that dome CD11c^hi lysozyme-expressing cells derive from CCR2+ monocytes and are composed of LysoDCs and two macrophage subsets. Conversely to villus macrophages, the latter do not express the classic macrophage markers F4/80, CD64 (Fc Gamma Receptor I), CD169 (sialoadhesin), and CD206 (mannose macrophage receptor). Unlike dome macrophages, LysoDCs have a

rapid turnover and can efficiently prime naive T cells toward a Th1 phenotype in vitro.

RESULTS

Phenotypic Distinction between Mononuclear Phagocytes of the Dome and of the DAVs

PPs are constituted of dome and DAVs. A major issue when analyzing the MPS of the dome after isolation of cells from PPs is the presence of phagocytes extracted not only from the dome but also from the DAVs.

By confocal microscopy, most CX_3CR1-expressing phagocytes located in the SED and in the DAVs expressed CD11c and SIRPα, but could be distinguished by the specific expression of F4/80 and CD169 in the DAVs and of lysozyme in the SED (Figures 1A–1C). CD169 also was expressed by macrophages at the base of the IFR (Figure S1A), whereas F4/80$^+$ cells were either rare or absent in the whole dome (Table S1). Thus, according to these confocal microscopy data, we could establish a flow cytometry gating strategy to distinguish PP phagocytes of the dome from those of DAVs based on their F4/80 and lysozyme differential expression. To confirm this issue, we compared CD11c$^+$ cells isolated from either villi or PPs (Figure 1D). Unlike commonly used methods, we applied short digestion time without prior EDTA treatment before magnetic sorting of CD11c$^+$ cells to avoid as much as possible the release of DAV cells (Figure S1B). Using these conditions, lysozyme-expressing cells were specifically detected in the CX_3CR1^{hi} gate of PP cells, but not in the villi (Figure 1D, P_1; Figure S1B), confirming the absence of PPs in the villus fraction and the specific location of lysozyme-expressing cells in the dome. The high number of F4/80^{hi} cells in the PP fraction indicated that an important part of the collected CD11c$^+$ cells were issued from DAVs (Figure 1D, P_2). Importantly, dome lysozyme-expressing cells expressed similar levels of CX_3CR1 as CX_3CR1^{hi}F4/80^{hi} DAV phagocytes, but higher levels of CD11c (Figure 1D; Figure S1B). The combination of SIRPα and CD11b markers on the CD11c^{hi} fraction of cells (Figure 1D, P_3) allowed us to distinguish DAV DCs, expressing high levels of CD11b and intermediate levels of SIRPα (Figure 1D, P_4), from dome phagocytes, expressing either higher levels of SIRPα (Figure 1D, lysozyme-expressing cells, P_1) or no or lower levels of CD11b (Figures 1D and S1C, dome DN, CD11b$^+$, and CD8α$^+$ DCs identified as P_5, P_6, and P_7, respectively). Finally, CD11c^{hi} lysozyme-expressing cells could be split into two subpopulations according to their MHCII surface expression (Figure 1D, last column). Thus, the MPS of DAVs (P_2 and P_4) and dome (P_1, P_5, P_6, and P_7) can be distinguished based on a combination of markers, including CD11c, F4/80, CD11b, and SIRPα.

Circulating Monocytes Give Rise to Both LysoDCs and Macrophages in PPs

In the gut, CX_3CR1^{hi} cells are mostly derived from Ly6C^{hi}CCR2$^+$-circulating monocytes (Bogunovic et al., 2009; Varol et al., 2009). The egress of these monocytes from the bone marrow (BM) into the blood is largely dependent on the chemokine receptor CCR2, and CCR2-deficient mice show a drastically reduced number of circulating Ly6C^{hi} monocytes (Serbina and Pamer, 2006). Given that dome lysozyme-expressing cells were CX_3CR1^{hi} (Figure 1D),

we investigated whether their number was altered in CCR2-deficient mice. Surprisingly, we noticed that MHCII^{hi} lysozyme-expressing cells were strongly reduced in CCR2-deficient mice, while those expressing low levels of MHCII were slightly or not altered (Figures 2A and 2B). The latter were the only ones to express CD4 (Figure 2A). Moreover, as they strongly displayed autofluorescence (AF), they most likely corresponded to macrophages and were thus termed LysoMacs, whereas the CD11c^{hi}MHCII^{hi}CD4$^-$AF$^{lo/int}$ cells were considered as LysoDCs.

Because our attempts to detect cells derived from transferred monocytes into $Ccr2^{-/-}$ mouse PPs were unsuccessful, we reconstituted lethally irradiated CD45.1$^+$CD45.2$^+$ mice with a 1:1 mixture of BM cells isolated from wild-type (WT) CD45.1$^+$ mice and either CD45.2$^+Batf3^{-/-}$ or CD45.2$^+Ccr2^{-/-}$ mice. As expected, we found that LysoDCs derived mostly from $Ccr2^{+/+}$ precursors, while dome CD8α$^+$, CD11b$^+$, and DN DCs consisted of both $Ccr2^{+/+}$ and $Ccr2^{-/-}$ donor cells (Figure 2C). Interestingly, although LysoMacs were only slightly altered in CCR2-deficient mice (Figure 2B), they mainly derived from $Ccr2^{+/+}$ precursors, too (Figure 2C). Moreover, LysoDCs and LysoMacs developed irrespective of the presence of $Batf3$, while dome CD8α$^+$ DCs derived mainly from $Batf3^{+/+}$ donor cells (Figure 2C), confirming that Batf3 is required for the differentiation of dome CD8α$^+$ DCs (Hildner et al., 2008). Dome CD11b$^+$ and DN DCs derived preferentially but not exclusively from $Batf3^{-/-}$ precursors, which indicated that Batf3 deficiency could induce a competitive advantage toward the dome CD11b$^+$ and DN DC lineages. Altogether, these data support the monocytic origin of LysoDCs and LysoMacs and the common DC precursor (CDP) origin of dome CD8α$^+$, CD11b$^+$, and DN conventional DCs (cDCs).

Given that both LysoMacs and LysoDCs derived from CCR2$^{+/+}$ donor cells in competitive chimeric mice whereas only LysoDCs were strongly altered in CCR2$^{-/-}$ mice, we investigated whether this discrepancy could be explained by an embryonic origin and self-renewal of LysoMac through life as recently demonstrated for most tissue macrophages (Hashimoto et al., 2013; Schulz et al., 2012; Yona et al., 2013). Parabiosis between CD45.1 and CD45.2 mice was established for 2 months and the contribution of non-host-derived cells to LysoDCs, LysoMacs, and dome cDCs was assessed. Between 11% and 17% of dome cDCs and LysoDCs were of donor origin (Figure 2D). Similarly, exchange of blood-borne cells reached 12% for LysoMacs, indicating that circulating precursors contributed to the LysoMac population (Figure 2D). Moreover, when parabiosis was established between CCR2-deficient mice and WT mice, the $Ccr2^{-/-}$ parabionts contained 62% and 94% of donor cells for LysoMacs and LysoDCs, respectively, whereas chimerism was maintained below 16% for dome cDCs (Figure 2E), confirming that both LysoDCs and LysoMacs derived mainly from circulating monocytes.

The difference in CCR2 dependency between LysoDCs and LysoMacs might otherwise reflect differences in their renewal rate. We compared turnover times of DAV and dome DCs and macrophages using bromodeoxyuridine (BrdU) labeling. The renewal rate of LysoMacs was very slow and comparable to that of DAV macrophages, with less than 30% of cells being replaced by day 6 (Figure 2F). LysoDCs displayed a rapid turnover reaching 61% ± 9% of cell replacement at day 6 (Figure 2F). The
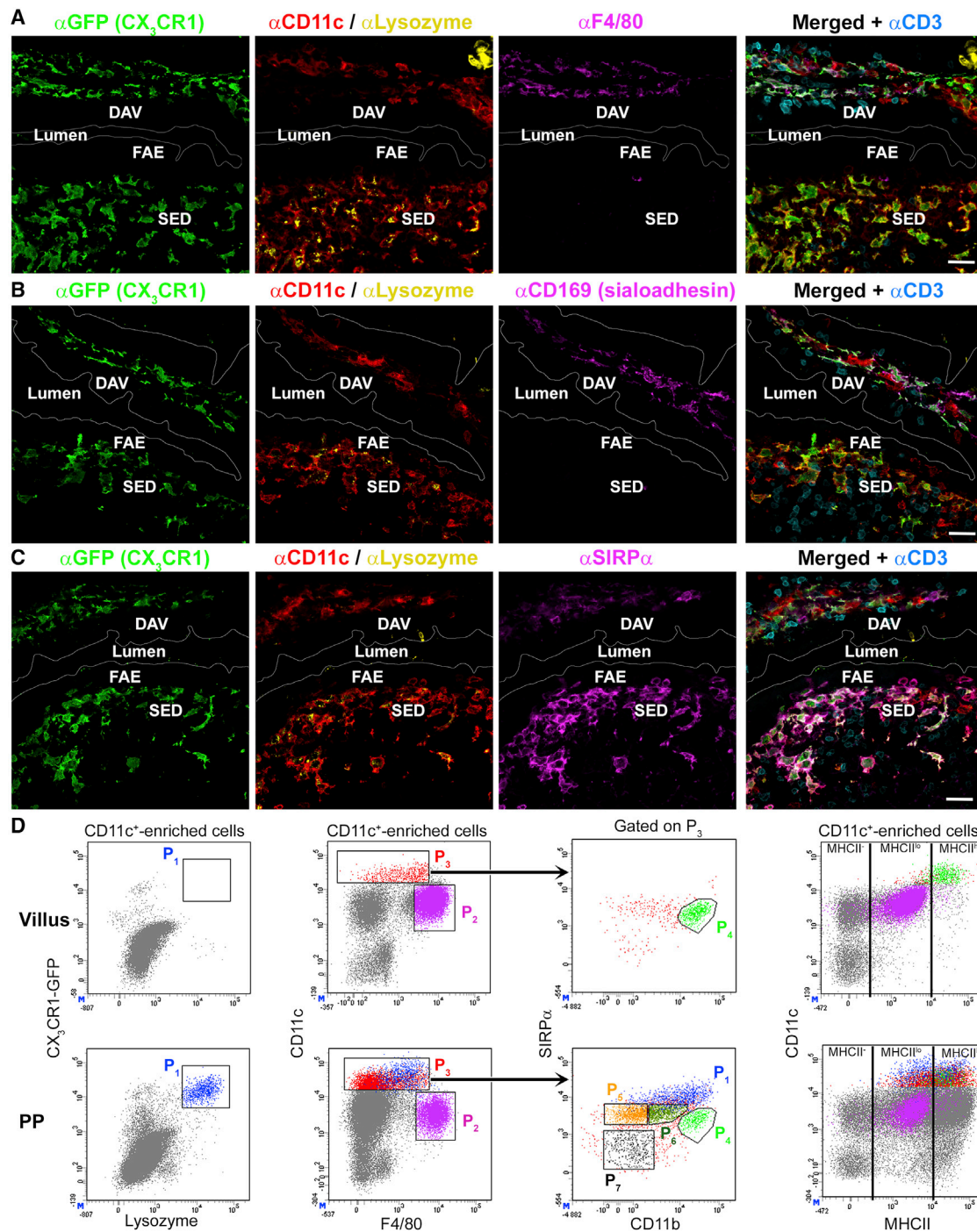
Figure 1. Phenotypic Distinction between Mononuclear Phagocytes of the Dome and of the DAVs

(A–C) Confocal microscopy projection of CX_3CR1-EGFP$^{-/+}$ mouse PP sections stained for EGFP (green), CD11c (red), lysozyme (yellow), CD3 (cyan), and (A) F4/80, (B) CD169, or (C) SIRPα (magenta). $CX_3CR1^+CD11c^+$ lysozyme$^+$ cells of the SED expressed SIRPα, but neither F4/80 nor CD169, whereas the DAV $CX_3CR1^+CD11c^+$lysozyme$^-$ cells displayed all three markers. Bars, 20 μm.

(D) Flow cytometry analysis of villus and PP CD11c$^+$-enriched cells. (First column) CX_3CR1^{hi} lysozyme$^+$ cells were only detected in PPs (P_1). (Second column) Villus and DAV F4/80^{hi} cells (macrophages and eosinophils) expressed lower level of CD11c (P_2) than DCs (P_3). (Third column gated on P_3) Villus and DAV DCs (P_4) displayed lower levels of SIRPα than dome $CX_3CR1^{hi}CD11c^{hi}$ lysozyme$^+$ cells (blue, P_1) and higher levels of CD11b than dome DN (P_5), CD11b$^+$ (P_6), and CD8α^+ (P_7) DCs. (Last column) Dome $CX_3CR1^{hi}CD11c^{hi}$ lysozyme$^+$ cells (blue) expressed either high or low levels of MHCII. See also Figure S1. Data are representative of six independent experiments.

turnover rates of dome cDCs were even faster, reaching 92% ± 9% at day 6 (Figure 2F). Thus, LysoDC number may be reduced in CCR2-deficient mice due to their short lifespan and insufficient circulating precursors to replace them, whereas the slow turnover of LysoMacs may allow their replenishment by fewer blood monocytes.

Genetic Global Relationships among PP Phagocyte Subsets

To perform a transcriptomic analysis of LysoDCs to be compared to LysoMacs and to the dome CD11b^{+} cDCs, we needed to define a gating strategy to sort each CD11c^{hi} MHCII^{+} cell subset of the dome without intracellular staining of lysozyme. The pDCs were excluded based on their lower expression of CD11c (Figure 3A). Surprisingly, BST2, a classic pDC marker (Blasius et al., 2006), was found to be expressed at the surface of LysoDCs and LysoMacs (Figure 3A). Thus, LysoDCs and LysoMacs were separated from pDCs and cDCs based on CD11c and BST2 expression, respectively (Figure 3B). LysoDCs and LysoMacs were then separated using CD4 and MHCII expression (Figure 3B). Finally, dome CD11b^{+} cDCs were distinguished from dome DN and CD8α^{+} cDCs and DAV DCs with CD8α and the same combination of CD11b and SIRPα staining, as shown in Figure 1D.

Triplicates of LysoDCs, LysoMacs, and dome CD11b^{+} cDCs were analyzed by whole-mouse genome microarray. LysoDCs and LysoMacs clustered separately from dome CD11b^{+} cDCs (Figure S2A), and 106 differentially expressed genes were found between LysoDCs and LysoMacs, whereas more than 850 genes distinguished dome CD11b^{+} cDCs from LysoMacs or LysoDCs (Figure S2B). As expected, the main genes selectively expressed in the CDP-differentiation pathway (i.e., *Flt3*, *Zbtb46*, and *Id2*) were weakly or not expressed in LysoDCs and LysoMacs, while those of the monocyte/macrophage pathway of differentiation (i.e., *Csf1r* and *Mafb*) were strongly expressed (Figure S2C). Moreover, there was an increase or decrease of the proportion of LysoDCs and LysoMacs among CD11c^{hi}MHCII^{+} cells upon treatment of mice with inhibitors of Flt3 (Quizartinib) or CSF1 receptor (GW2580), respectively (Figure S2D). This confirmed LysoDC and LysoMac dependency on CSF-1 receptor, but not Flt3 signaling. In addition to *Mafb*, other transcription factor genes typically associated with monocyte gene signature also were enriched in LysoDCs and LysoMacs (Figure S2E).

As expected, *Ccr2* and *Cx3cr1* were mainly expressed by LysoDCs and LysoMacs, whereas *Ccr6* and *Ccr7* were mostly expressed by dome CD11b^{+} cDCs (Figure S2E). There was also a differential expression of genes encoding cytokines (*Il1a* and *Tnfsf13b* enriched in LysoDCs and LysoMacs, *Il1b* in LysoDCs and CD11b^{+} cDCs, *Il6* and *Tnfsf9* in CD11b^{+} cDCs, and *Tnfsf15* in LysoMacs) and chemokines (*Cxcl10* enriched in LysoDCs and LysoMacs, *Ccl19* in LysoMacs, *Ccl22* in CD11b^{+} cDCs, and *Cxcl14* in LysoDCs) (Figure S2E).

PP Monocyte-Derived Cells Display Antibacterial and Antiviral Gene Signatures

BST2, which was used in our gating strategy to isolate LysoDCs and LysoMacs, is an antiviral protein known to be induced by type I interferon (IFN) and the transcriptional factor IRF7 (Bego

et al., 2012; Blasius et al., 2006). We thus investigated the expression of the IFN-signaling pathway genes. Type I IFN receptor genes (*Ifnar1* and *Ifnar2*), *Ikbke* (IKKe), *Irf7*, and *Irf8* were indeed upregulated in LysoDCs and LysoMacs compared to dome CD11b^{+} cDCs, whereas STAT and other IRF transcriptional factor genes showed either lower (*Irf4/5* and *Stat4/5a*) or no differential expression (Figure 3C). Functional association network analysis revealed that IRF7-associated genes also were enriched in LysoDCs and LysoMacs (Figure 3D). *Ikbke* and *Irf7* both have been reported to be master regulators of IFN-dependent antiviral immune responses (Honda et al., 2005; Tenoever et al., 2007). Actually, genes encoding molecules participating in the recognition of virus, such as *Ddx58* (RIG-I), *Ddx60*, *Ifi204* (IFI16), *Tlr7*, *Tlr9*, *Tmem173* (STING), and *Zbp1* (DAI) (Aoshi et al., 2011), as well as other IFN-stimulated genes with previously well-described antiviral activity, such as *Bst2*, *Gbp*, *Ifit*, *Oas*, *Oasl*, *Rnase l*, and *Rsad2* (viperin) (Sadler and Williams, 2008; Schoggins and Rice, 2011), were upregulated in LysoDCs and LysoMacs (Figure 3E), indicating that monocyte-derived cells may be key players in the innate immune response against viral infection in PPs.

LysoDCs and LysoMacs were also better equipped to respond to bacterial infection than dome CD11b^{+} cDCs. They were enriched in bacterial-sensing (*Tlr* and *Naip*) genes as well as antibacterial immunity-related genes, such as *Aoah* (acyloxyacyl hydrolase), *Irg1*, and *Lyz1* (lysozyme P) (Figure 3F). LysoDCs and LysoMacs were also strongly enriched in genes associated with transition metal transport and sequestration, a mechanism of host defense against bacterial infection known as nutritional immunity (Hood and Skaar, 2012; Figure 3F). Among them, *Hamp* (hepcidin), *Hp* (haptoglobin), and *Tfrc* (transferrin receptor) were specifically enriched in LysoDCs, whereas *Slc11a1* (NRAMP1) and *Slc40a1* (ferroportin) were upregulated in LysoMacs, indicating distinct mechanisms of iron availability regulation for LysoDCs and LysoMacs.

Altogether these data indicate that LysoDCs and LysoMacs, but not dome CD11b^{+} cDCs, display strong innate defense mechanisms against viral and bacterial infections.

LysoDCs Display the Functional Gene Signature of a Non-inflammatory Monocyte-Derived DC

Recognition of pathogens also occurs through C-type lectin receptors (CLRs) (Sancho and Reis e Sousa, 2012). Several CLR genes were selectively expressed either by LysoMacs (*Clec1b* and *Clec7a* encoding Dectin-1; Figure 4A) or by LysoDCs (*Clec4a1*, *Clec4a2*, and *Clec4n* encoding Dectin-2; Figure 4A). Actually, the top 20 of LysoDC-upregulated genes versus LysoMac included three CLR-encoding genes, *Clec4a1*, *Clec4a2*, and *Clec4a4* (Figure 4B). CLEC4A4/DCIR2 is a classic CD11b^{+} cDC marker recognized by the 33D1 antibody (Dudziak et al., 2007). Its expression by LysoDCs and dome DN and CD11b^{+} cDCs, but not by LysoMacs or dome CD8α^{+} cDCs, was confirmed by flow cytometry (Figure 4C). We further checked the specificity of this gene by integrating the MPS gene expression data from the ImmGen project (Heng et al., 2008) and found that it was neither expressed by macrophages nor monocytes (Figure 4D). *Sucnr1,* which codes for the succinate receptor GPR91, also was found to be highly specific of LysoDCs and
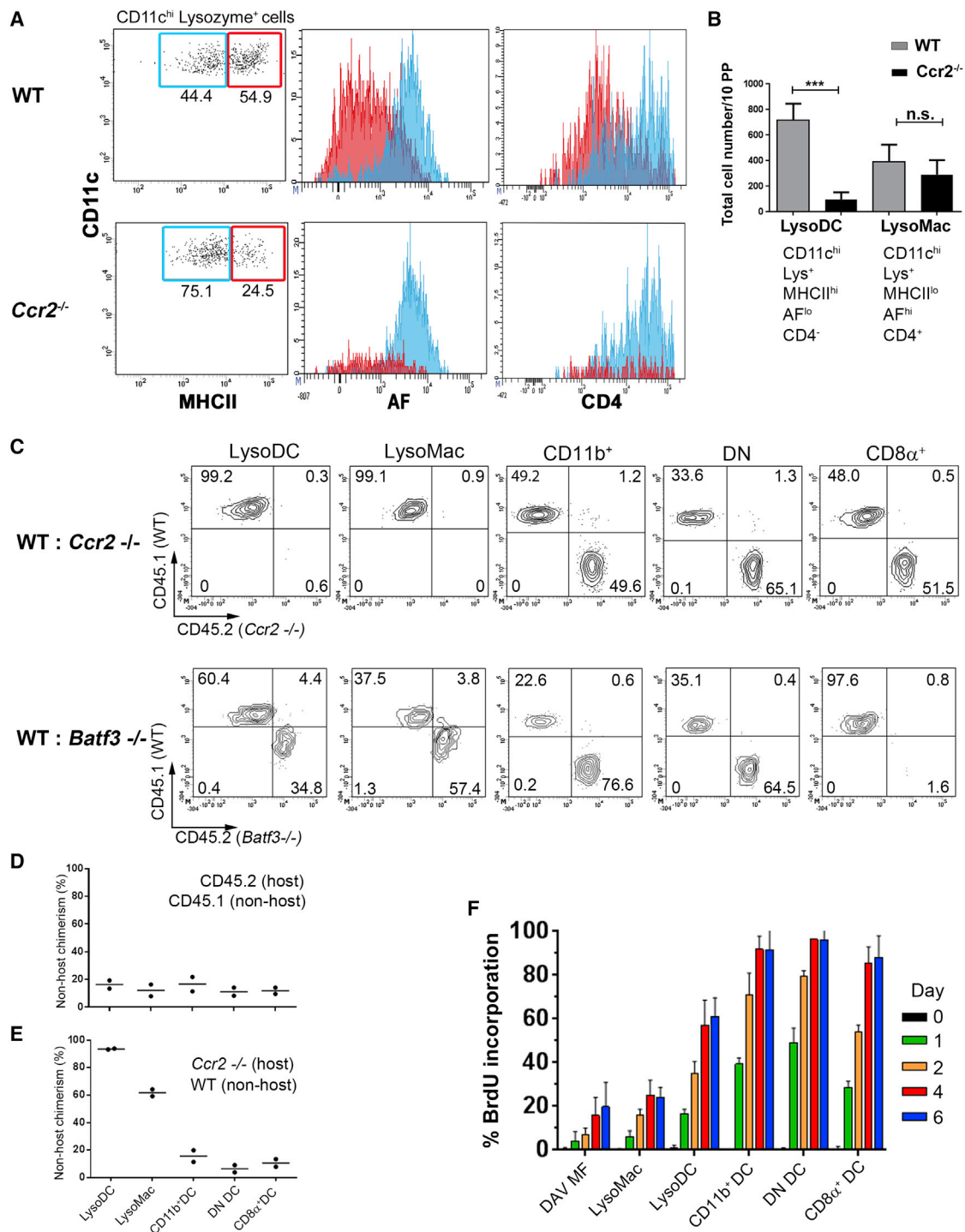
Figure 2. Dual Differentiation of Monocytes into LysoDCs and Macrophages

(A) AF and expression of CD4 was compared in PP MHCII^{lo} (blue) and MHCII^{hi} (red) CD11c^{hi} lysozyme^{+} cells of WT (top) and CCR2-deficient mice (bottom). LysoDCs, which were weakly autofluorescent lysozyme^{+} cells expressing high levels of MHCII, but no CD4, were strongly reduced in CCR2-deficient mice conversely to AF^{hi}MHCII^{lo}CD4^{+} lysozyme^{+} cells hereafter referred to as LysoMacs.

(B) Absolute numbers of LysoDCs and LysoMacs extracted from PPs of WT and CCR2$^{-/-}$ mice are shown (mean ± SD; ***p < 0.001, Student's t test).

(C) Expressions of CD45.1 and CD45.2 in the PP MPS of lethally irradiated CD45.1 × CD45.2 mice reconstituted with equal amounts of CD45.1^{+} WT and CD45.2^{+}Ccr2$^{-/-}$ or CD45.2^{+} Batf3$^{-/-}$ BM cells. LysoDCs and LysoMacs were derived specifically from CCR2-expressing cells and CD8α^{+} DCs from Batf3-expressing cells.

of a very restricted number of CD11b⁺ cDC subsets (mainly dome CD11b⁺ cDCs and spleen CD4⁺ cDCs; Figure 4D).

The top 20 of LysoDC-upregulated genes versus LysoMac also comprised four transcripts related to the MHCII presentation pathway (Figure 4B), among which *H2-Eb2* was not expressed by any macrophage or monocyte population of the ImmGen database (Figure S3A). Several other genes linked to this pathway also were upregulated in LysoDCs and dome CD11b⁺ cDCs (Figure S3B). These data indicated that LysoDCs are fully equipped to present antigens as efficiently as CD11b⁺ cDCs, while LysoMacs are not.

Finally, of the 71 LysoDC-upregulated genes as compared to LysoMac (Figure S2B), 51 also were upregulated in dome CD11b⁺ cDCs, among which 20 were known to be involved in DC functions and ten even belonged to the core DC signature, as defined by Miller et al. (Miller et al., 2012; Figure 4E). However, LysoDCs did not express the monocyte-derived inflammatory DC markers (Cheong et al., 2010; Serbina et al., 2003; Siddiqui et al., 2010): *Ly6c1* (Ly6C), *Cd209a* (DC-SIGN), *Cdh1* (E-Cadherin), *Nos2* (iNOS), or *Tnf* (Figure S3A). Moreover, LysoDCs displayed a similar distribution and were in comparable proportion among CD11cʰⁱMHCII⁺ cells in conventional and germ-free mice, which are devoid of any potential food and microflora-induced stimulus, confirming their non-inflammatory nature (Figure 4F). Thus, LysoDCs are fully differentiated monocyte-derived non-inflammatory cells, which differ from macrophages by a gene signature linked to DC functions.

Diversity and Distribution of PP Macrophages
Fcgrl (encoding CD64, the Fc Gamma receptor I), expressed virtually by all monocyte and macrophage populations (Gautier et al., 2012; Tamoutounour et al., 2012), was not expressed by LysoMacs (Figure S4). We also confirmed at the gene level the absence of F4/80 (*Emr1*) and CD169 (*Siglec1*), and we found that the other classic macrophage markers, CD14 and CD206 (*Mrc1*), were not expressed by LysoMacs, although present in villus macrophages (Figure S4). These data confirmed the atypical expression of genes in dome macrophages as compared to other tissue macrophages.

Cd4 and *Timd4* were the most upregulated transcripts in LysoMacs as compared to LysoDCs (Figures 5A and 5B). TIM-4, the phosphatidylserine receptor encoded by *Timd4* (Miyanishi et al., 2007), was expressed at the surface of half of the LysoMacs (Figure 5C). We took advantage of CD4 and TIM-4 as discriminative markers to study the distribution of LysoDCs and LysoMacs by microscopy. In addition to their main location, i.e., the SED, LysoDCs and LysoMacs were scattered throughout the follicle (Figure 5D; Figure S5A). TIM-4⁺ LysoMacs were located in the lower part of the follicle, whereas TIM-4⁻ LysoMacs were situated in the upper part and in the SED (Figure 5D). TIM-4⁺ LysoMacs also were present at the periphery and inside the IFR enriched in T cells (Figure 5E). We have shown previously

that tingible-body macrophages (TBMs) of the PP germinal centers (GCs) are devoid of most MPS surface markers, such as CD11c, CD11b, F4/80, CD169, and MHCII (Lelouard et al., 2010). Here we observed that TBMs displayed CD4 and TIM-4 on their surface (Figure 5F). PP serosal macrophages were also CD4⁺TIM-4⁺ (Figure 5F; Table S1). Finally, DAV macrophages expressed CD4. Thus, CD4 seems to be a general surface marker of small intestine macrophages.

Altogether, our data identified five different CD4⁺ macrophage subsets in PPs: TIM4⁺ TBMs in the GC, CD169⁺TIM-4⁺ and CD169⁻TIM-4⁺ serosal macrophages, TIM-4⁻ LysoMacs in the SED and the upper part of the follicle, and, lastly, TIM-4⁺ LysoMacs in the IFR and the lower part of the follicle (Table S1).

Both LysoDCs and TIM-4⁻ LysoMacs Are Involved in Particulate Antigen Uptake and, upon TLR7 Stimulation, Secrete IL-6 and TNF
Lysozyme-expressing cells previously were identified as the main particulate antigen and pathogenic bacteria-sampling cells in the SED (Lelouard et al., 2010, 2012). However, no distinction was made between LysoDCs and LysoMacs. Here we found that CX₃CR1 was not required for the formation of trans-M cell dendrites and that most lysozyme-expressing cells extending these dendrites did not express CD4 (40 CD4⁻ cells among 50 lysozyme-expressing cells extending dendrites examined; Figure S5B), indicating that these cells were mainly LysoDCs. Nevertheless, TIM-4⁻ LysoMacs, but neither cDCs nor other SED cells, were able to internalize microspheres administrated orally as efficiently as LysoDCs (Figure 6A).

We next investigated the ability of LysoDCs and LysoMacs to upregulate MHCII and costimulatory molecules and secrete cytokines upon in vitro stimulation with R848, an agonist for TLR7 whose gene was strongly enriched in LysoDCs and LysoMacs as compared to dome CD11b⁺ cDCs (Figure 3E). Upon stimulation, expression of MHCII, CD40, and CD86 increased at the surface of LysoDCs, whereas only a slight but not significant increase of CD40 and CD86 was observed for LysoMacs (Figure 6B). TLR7 activation also induced IL-6 and TNF secretion by LysoDCs and to a lesser extent by LysoMacs, whereas no IL-10 or IFNγ production was observed for any subset (Figure 6C).

Unlike LysoMacs, LysoDCs Efficiently Prime Naive Helper T Cells to Induce a Th1 Immune Response
To determine whether LysoDCs or LysoMacs could interact with and prime naive helper T (Th) cells, each dome DC subset and LysoMacs were isolated, pulsed with ovalbumin (OVA), and co-cultured with naive OVA-specific Th cells (Barnden et al., 1998). Strikingly, after 16 hr of co-culture, strong interactions between LysoDCs and naive Th cells were observed, whereas only phagocytized Th cells could be seen for LysoMacs (Figure 6D; Movies S1, S2, and S3). Moreover, the number of Th cells

---

(D and E) Parabiotic pairs were generated from CD45.1⁺ and either (D) CD45.2⁺ WT mice or (E) *Ccr2*⁻/⁻ mice. The percentage of non-host cells among each PP MPS subset was determined 2 months after surgery. LysoDCs and LysoMacs were derived from CCR2-dependent circulating precursors.

(F) Kinetics of BrdU labeling administrated to mice for 6 days. LysoDCs reached 61% of BrdU incorporation at day 6, whereas DAV macrophages and LysoMacs barely reached 30%. Results are shown as mean ± SD. Data are from two (D and E) to three independent experiments (A, B, C, and F), with pooled cells from three to six mice per experiment.
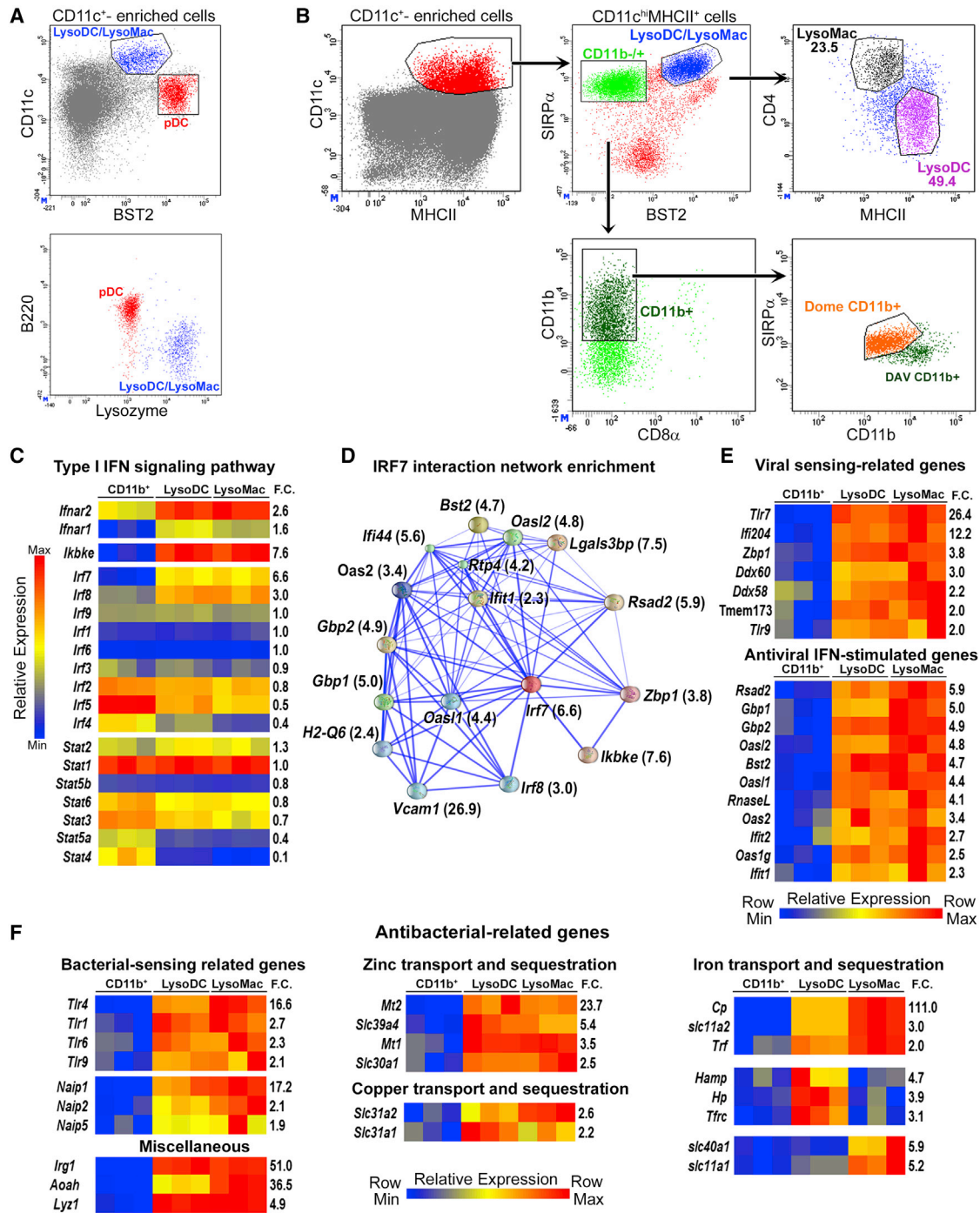
Figure 3. PP Monocyte-Derived Cells Express BST2 and Display Strong Innate Antiviral and Antibacterial Gene Signatures

(A) Surface expression of CD11c and Bst2 (top) allowed us to distinguish LysoDCs/LysoMacs (blue) from other CD11c^{hi} cells (gray) and from pDC (red), as confirmed by B220 and lysozyme staining (bottom).

(B) Gating strategy for LysoDC, LysoMac, and dome CD11b^{+} cDC sorting is shown.

(C) Heatmap of the type I IFN-signaling pathway and associated transcription factor gene expression in dome CD11b^{+} cDCs, LysoDCs, and LysoMacs. Type I IFN receptor (IFNAR1 and IFNAR2), IκB kinase ε, IRF7, and IRF8 gene expression was upregulated in LysoDCs and LysoMacs as compared to dome CD11b^{+} cDCs. Fold change (F.C.) is indicated on the right.

(D) Confidence view shows the IRF7 functional association network upregulated in LysoDCs and LysoMacs as compared to dome CD11b^{+} cDCs (fold change indicated in brackets) using String 9.1 database with *Bst2* and *Irf7* as input nodes.

(E and F) Heatmaps illustrate the upregulation of viral sensing (E, top), antiviral (E, bottom), and antibacterial (F) genes in LysoDCs and LysoMacs as compared to dome CD11b^{+} cDCs. See also Figure S2. Data are from three independent cell-sorting experiments with pooled cells from 42 mice per experiment.
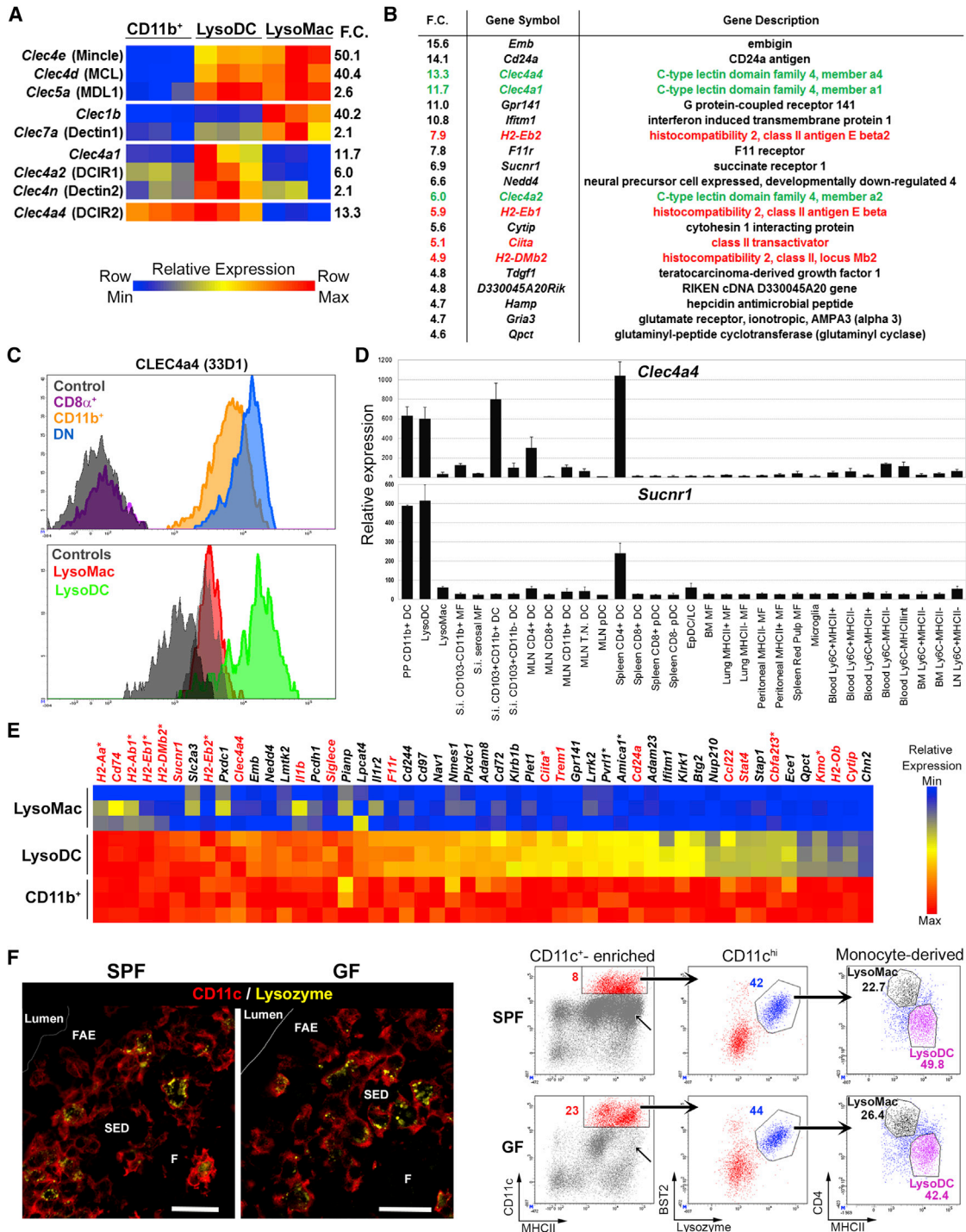
Figure 4. LysoDCs Are Non-inflammatory Monocyte-Derived Cells with a Gene Signature Linked to DC Functions

(A) Heatmap shows CLR genes with differential expression between monocyte-derived cells and dome CD11b^{+} cDCs, LysoMacs or LysoDCs and the other two subsets, and finally DCs and LysoMacs. Fold change (F.C.) is indicated on the right.

(B) Top 20 of LysoDC-upregulated genes as compared to LysoMac. MHCII presentation pathway and CLR genes are in red and green, respectively.

(C) Surface expression of CLEC4A4 in dome CD8α^{+} (magenta), CD11b^{+} (orange), and DN (blue) cDCs, and in LysoMacs (red) and LysoDCs (green). Isotype control staining (gray) allowed us to appreciate the high AF of LysoMacs.

(D) Normalized mean relative expression ± SD of *Clec4a4* and *Sucnr1* in the MPS of different tissues. Data are taken from the ImmGen database (Heng et al., 2008).

(legend continued on next page)

interacting with LysoDCs increased when LysoDCs were stimulated with R848 (Figure 6D; Movies S4 and S5).

After 5 days of co-culture, LysoDCs and dome cDC subsets induced naive Th cell proliferation efficiently, whereas LysoMacs did not (Figure 7A). When stimulated with R848, LysoDCs significantly increased their ability to induce Th cell proliferation, whereas weak Th cell proliferation was observed with stimulated LysoMacs. Altogether, our results indicate that unlike LysoMacs, LysoDCs can process antigens adequately and prime naive Th cells efficiently.

We then addressed the polarization of primed Th cells by intracellular flow cytometry and cytometric bead array (Figures 7B and 7C; Figure S6). Only background levels of secreted IL-4, IL-10, and IL-17 were monitored (Figure 7C; Figure S6). Production of IL-2 was induced by all DC subsets and, only after TLR7 stimulation, by LysoMacs (Figure S6). In accordance with a previous report (Sato et al., 2003), dome CD11b+ cDCs induced IL-6 production, but no TNF or IFNγ (Figures 7B and 7C). A similar profile of secretion was obtained for Th cells co-cultured with dome DN cDCs (Figures 7B and 7C). LysoDCs and dome CD8α+ cDCs primed naive Th cells to secrete IFNγ (Figure 7B). This production was further increased upon R848 stimulation. Finally, R848 also promoted the production of IL-6 and TNF in the supernatants of Th cells co-cultured with LysoDCs and, to a lesser extent, with LysoMacs (Figure 7C). Thus, LysoDCs efficiently prime naive Th cells to induce a Th1 immune response, which is further amplified upon TLR7 stimulation.

DISCUSSION

In this study, we determined the phenotype, distribution, origin, lifespan, and function of the PP MPS. Although monocyte-derived DCs are widely used in vitro, their equivalent in vivo mostly has been demonstrated in inflammatory conditions (Cheong et al., 2010; Serbina et al., 2003), and whether monocytes can give rise to DCs in the absence of inflammation still remains a matter of debate (Geissmann et al., 2010; Hashimoto et al., 2011; Jakubzick et al., 2013; Satpathy et al., 2012; Tamoutounour et al., 2013). Our results indicate that LysoDCs are derived from monocytes. They express transcription factors and growth factor receptors related to the monocyte, but not to the CDP pathway of differentiation. Thus, they do not express Flt3, which is required for cDC development in vivo (Bogunovic et al., 2009; Ginhoux et al., 2009; Varol et al., 2009; Waskow et al., 2008). Moreover, they are dependent on M-CSF, the growth factor involved in monocytic progeny differentiation, and on CCR2, the chemokine receptor that permits monocyte egress from the BM (Serbina and Pamer, 2006). However, their presence does not rely on microbial stimulation.

Morphologically, LysoDCs are large stellate motile cells (Lelouard et al., 2010, 2012) that display some of the phenotypical and functional characteristics of DCs. Phenotypically, in addition to high level expression of CD11c and MHCII, they display the 33D1 antigen, CLEC4A4, which was the first specific mouse DC marker to be described (Dudziak et al., 2007; Nussenzweig et al., 1982). LysoDCs also express the succinate receptor GPR91, whose expression in the MPS is restricted to a few CD11b+ DC subsets. Interestingly, GPR91 is involved in sensing danger, and, upon succinate triggering, promotes the migration of DCs, their production of proinflammatory cytokines, and their ability to prime Th cells (Rubic et al., 2008).
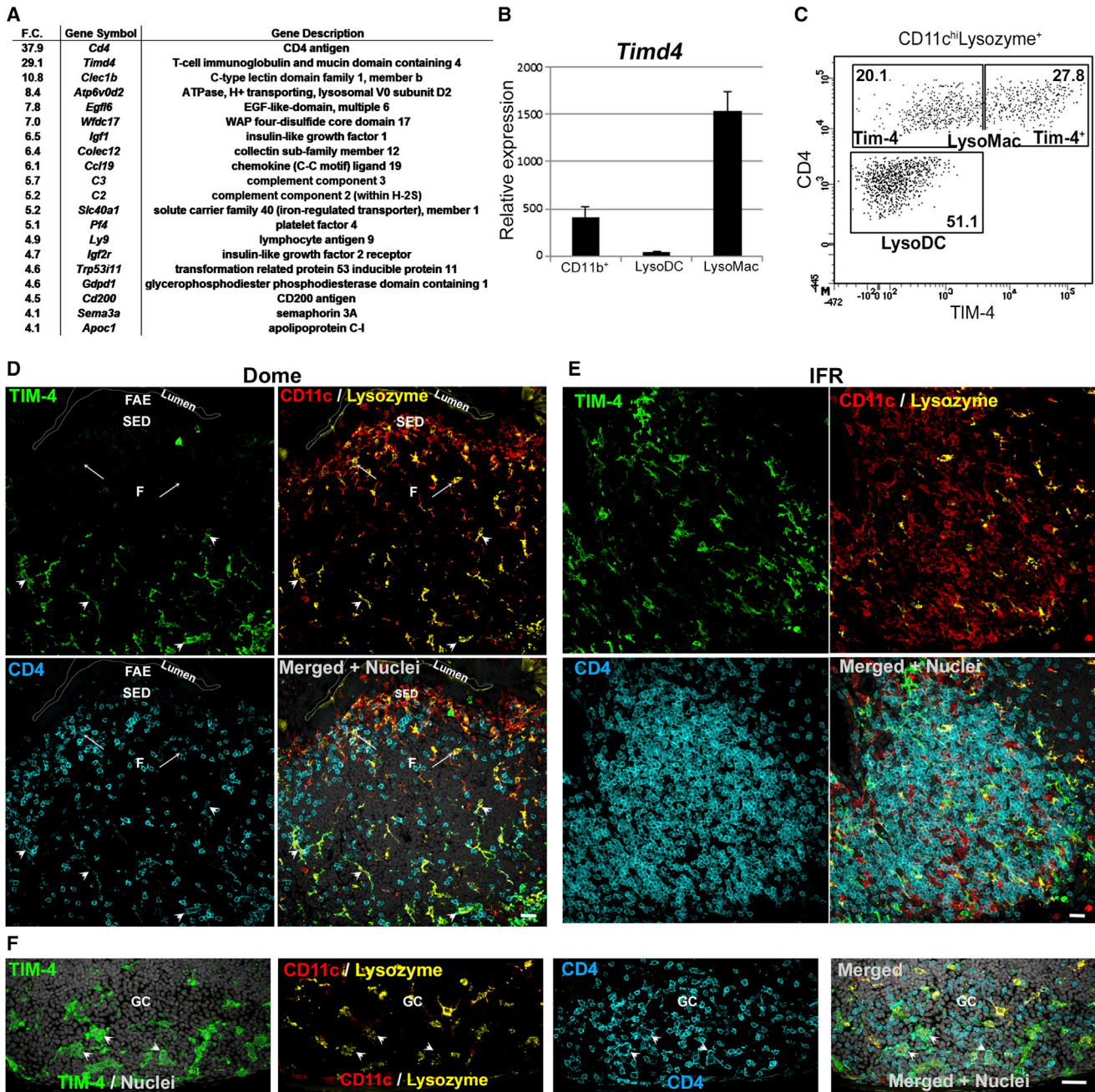
In addition to these DC phenotypic features, we also demonstrate that they have a short half-life and are able to prime naive Th cells in vitro for IFNγ production. However, LysoDCs do not express the chemokine receptor CCR7, which is required for cDCs to migrate into T cell zones for antigen presentation. Since the SED also is enriched in B and Th cells, CCR7-dependent migration may not be required for antigen presentation in PPs. It has now to be determined whether LysoDCs can prime effector cells in vivo at this site of antigen uptake. Upon TLR7 activation, LysoDCs secrete IL-6 and TNF and induce a higher production of IFNγ by Th cells. IL-6 is a cytokine known to play a major role in the development of IgA-secreting B cells (Ramsay et al., 1994; Sato et al., 2003). Previous reports have shown that PP DCs and especially CD11b+ DCs are implicated in the differentiation of naive B cells into IgA-producing plasma cells (Mora et al., 2006; Sato et al., 2003). It remains to be established whether these CD11b+ DCs are LysoDCs or dome CD11b+ cDCs. In summary, LysoDCs are steady-state monocyte-derived cells with DC morphology, phenotype, and function.

Interestingly, in PPs, monocytes also can give rise to CD4+ cells that display the characteristics of macrophages, i.e., long-lived cells with strong phagocytic activity but poor naive T cell-priming ability. Therefore, CD11chi lysozyme-expressing cells are composed of two main subpopulations: LysoDCs, which express CLEC4A4, high levels of MHCII, but no CD4; and LysoMacs, which express CD4, low levels of MHCII, and no CLEC4A4. In our previous studies, we could not distinguish LysoMacs from LysoDCs and they were collectively termed LysoDCs (Lelouard et al., 2010, 2012). We show here that, although the trans-M cell sampling of luminal antigen by CD11chi lysozyme-expressing cells is mainly mediated by LysoDCs, LysoMacs can internalize particulate antigens very efficiently too, probably after luminal antigen transport by M cells. Both LysoDCs and LysoMacs display strong innate antiviral and antibacterial gene signatures, which is consistent with the fact that, as the first line of mononuclear phagocytes, they may have to deal with many different kinds of pathogens. Half of

---

(E) Heatmap shows LysoDC-upregulated genes as compared to LysoMac, for which expression also was upregulated in CD11b+ dome cDCs (51 of the 71 genes with a fold change >2 between LysoDCs and LysoMacs using the min/max method, see Figure S2B). Genes involved in DC functions are in red. *Genes of the cDC gene signature (Miller et al., 2012).

(F) Similar proportion and distribution of LysoDCs in specific pathogen-free (SPF) and germ-free (GF) mice. (Left) Confocal microscopy of PP cryostat section shows LysoDCs/LysoMacs (CD11c in red, lysozyme in yellow) in the SED of SPF and GF mice. (Right) Flow cytometry analysis shows that the ratio of monocyte-derived cells among CD11chi cells as well as the ratio of LysoDCs among monocyte-derived cells were similar in SPF and GF mice. Note the loss of an important population of CD11cintMHCIIhi cells (arrow) identified as B cells (B220+BST2− cells, not shown) in GF mice. Results are representative of three independent experiments with pooled cells from six mice per experiment. Bars, 20 μm. See also Figure S3.

A

F.C.	Gene Symbol	Gene Description
37.9	Cd4	CD4 antigen
29.1	Timd4	T-cell immunoglobulin and mucin domain containing 4
10.8	Clec1b	C-type lectin domain family 1, member b
8.4	Atp6v0d2	ATPase, H+ transporting, lysosomal V0 subunit D2
7.8	Egfl6	EGF-like-domain, multiple 6
7.0	Wfdc17	WAP four-disulfide core domain 17
6.5	Igf1	insulin-like growth factor 1
6.4	Colec12	collectin sub-family member 12
6.1	Ccl19	chemokine (C-C motif) ligand 19
5.7	C3	complement component 3
5.2	C2	complement component 2 (within H-2S)
5.2	Slc40a1	solute carrier family 40 (iron-regulated transporter), member 1
5.1	Pf4	platelet factor 4
4.9	Ly9	lymphocyte antigen 9
4.7	Igf2r	insulin-like growth factor 2 receptor
4.6	Trp53i11	transformation related protein 53 inducible protein 11
4.6	Gdpd1	glycerophosphodiester phosphodiesterase domain containing 1
4.5	Cd200	CD200 antigen
4.1	Sema3a	semaphorin 3A
4.1	Apoc1	apolipoprotein C-I

B *Timd4*

C CD11c^{hi}Lysozyme$^+$

D Dome

E IFR

F

Figure 5. Phenotype and Distribution of PP Macrophages

(A) Top 20 of LysoMac-upregulated genes as compared to LysoDC are shown.

(B) Normalized mean relative expression ± SD of *Timd4* in LysoDCs, LysoMacs, and dome CD11b$^+$ cDCs is shown.

(C) Surface expression of TIM-4 in CD11c^{hi} lysozyme$^+$ cells is shown.

(D–F) Confocal microscopy projections of a C57Bl/6 mouse PP section stained for TIM-4 (green), CD11c (red), lysozyme (yellow), and CD4 (cyan). (D) LysoMacs (CD11c$^+$CD4$^+$ lysozyme$^+$ cells) of the lower part of the follicle (arrowheads) expressed TIM-4, whereas LysoMacs of the SED and of the upper part of the follicle (arrows) did not. (E) LysoMacs of the IFR expressed TIM-4. (F) TBMs of the GC, which contained many apoptotic bodies (arrowheads; condensed nuclear material, and apoptotic bodies in gray), expressed lysozyme, CD4, and TIM-4, but not CD11c. Data are representative of five independent experiments. Bars, 20 μm. See also Figure S4.

LysoMacs display at their surface TIM-4, a phosphatidylserine receptor (Miyanishi et al., 2007). The distribution of TIM-4$^+$ macrophages correlates well with their proposed function in apoptotic effector cell clearance (Albacker et al., 2010, 2013), since TIM-4$^+$ LysoMacs and TBMs are located in zones of effector cell priming and selection, i.e., IFRs for T cells and
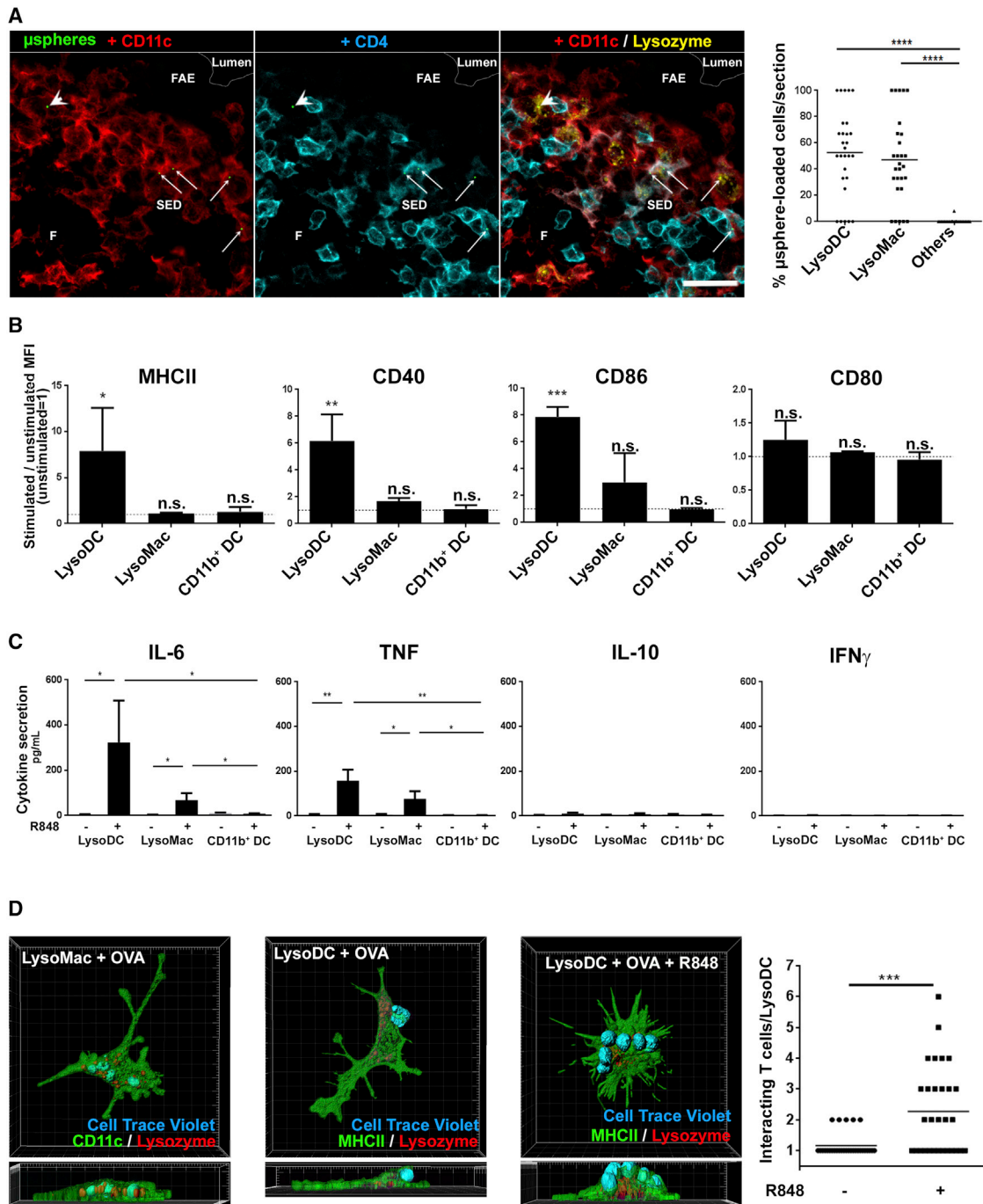
Figure 6. Uptake of Particulate Antigens and TLR7 Activation Features of PP Monocyte-Derived Cells

(A) Unlike dome cDCs, LysoDCs and LysoMacs internalized microspheres efficiently. (Left) Confocal microscopy shows PPs from a C57BL/6 mouse fed with 0.2 μm Yellow Green microspheres for 24 hr (green) and stained for CD11c (red), lysozyme (yellow), and CD4 (cyan). In the SED, microspheres were internalized by LysoDCs (arrowhead) and LysoMacs (arrows). Bar, 20 μm. (Right) Percentages of LysoDCs, LysoMacs, and other SED cells that had engulfed microspheres are shown. Quantitation was performed on three sections of two domes of two to three PPs for each of three mice (****$p < 0.0001$, one-way ANOVA followed by Bonferroni).

(B) Fold changes of MHCII and co-stimulatory molecules median fluorescence intensity (MFI) in LysoDCs, LysoMacs, and dome CD11b^{+} cDCs cultured for 24 hr with (stimulated) or without R848 (unstimulated, dashed line) are shown (n.s., non-significant; *$p < 0.05$, **$p < 0.01$, ***$p < 0.001$, one-way ANOVA followed by Bonferroni).

(C) IL-6, IL-10, TNF, and IFNγ secretions in the supernatant of LysoDCs, LysoMacs, and dome CD11b^{+} cDCs cultured for 24 hr with or without R848 were determined by cytometric bead array (*$p < 0.05$, **$p < 0.01$, Student's t test).

(legend continued on next page)

GCs for B cells. Therefore, we propose a model in which part of the pathogens entering through M cells would be destroyed by TIM4⁻ LysoMacs using their prominent innate defense mechanisms, while the other part would be killed and processed by LysoDCs to be presented to Th cells to mount a mucosal immune response. This response would be then regulated at the level of the GC and the IFR by TBM and TIM-4⁺ LysoMacs, respectively.

Collectively, our results show that, in the same microenvironment, monocytes develop into two closely related cell types with different lifespan and functional properties. These monocyte-derived cells differ greatly from their villous counterparts, as evidenced by their lack of expression of most classic intestinal macrophage markers. This indicates that the microenvironment of the dome exerts a strong influence on the differentiation program of monocytes. This strong imprinting pattern possibly reflects the crucial role of PPs in the mucosal immune response initiation, and future studies of the genes specifically expressed by the PP MPS will likely help to understand the mechanisms and pathways involved in this process.

EXPERIMENTAL PROCEDURES

Antibodies
Antibodies used are listed in the Supplemental Experimental Procedures.

Animals
The 6- to 10-week-old C57BL/6 and OT-II mice were from Charles River Laboratories. $Ccr2^{-/-}$ and $Cx_3cr_1^{GFP}$ mice have been described previously (Boring et al., 1997; Jung et al., 2000). All experiments were done in accordance with French and European guidelines for animal care.

Parabiosis
Parabiotic mice were generated from age- and weight-matched CD45.1⁺ (C57BL/6) and CD45.2⁺ (C57BL/6 or CCR2−/−) mice that were between 6 and 10 weeks old.

Generation of BM Chimera
The 6- to 10-week-old C57BL/6 (CD45.1 × CD45.2) mice were lethally irradiated with two doses of 4 Gy each, 4 hr apart, and then injected intravenously (i.v.) with at least 2.10⁶ BM cells obtained from femurs and tibias of CD45.1 (C57BL/6) and CD45.2 ($Ccr2^{-/-}$ or $Batf3^{-/-}$) mice. Then, 8 weeks after reconstitution, the level of chimerism was determined.

Chemical Treatments
The drinking water of mice injected intraperitoneally (i.p.) with 1.5 mg BrdU (Sigma-Aldrich) to ensure its immediate availability was supplemented for 1, 2, 4, and 6 days with 0.8 mg/ml BrdU. Mice were injected i.p. with 300 μg Quizartinib (LC Laboratories), 2 × 400 μg GW2580 (LC Laboratories), or 10% DMSO for 6 days before PP collection.

PP Cell Extraction
PPs were digested for 40 min at room temperature with collagenase/DNase as previously described (Lelouard et al., 2010). All subsequent procedures were at 0°C–4°C. CD11c⁺ cells were sorted using anti-CD11c microbeads and an AutoMACS magnetic cell separator according to the manufacturer's instructions (Miltenyi Biotec).

Flow Cytometry and Cell Sorting
CD11c⁺ were preincubated on ice for 10 min with the 2.4G2 antibody to block Fc receptors, stained for surface markers, and then permeabilized for BrdU and lysozyme labeling according to the manufacturer's protocol (BrdU-labeling Flow kit, BD Biosciences). Cell viability was evaluated using Fixable Viability Dye eFluor 506 (eBiosciences). Multiparameter flow cytometry and cell sorting were performed using a FACS LSRII and a FACSAria III (BD Biosciences), respectively. Data were analyzed with the BD FACSDiva software (BD Biosciences).

RNA Isolation and Microarray Analyses
The total RNA of PP-sorted MPS cells from three independent experiments was extracted with a QIAGEN micro RNAeasy PLUS kit. Quantity, quality, and absence of genomic DNA contamination were assessed with a Bioanalyser (Agilent Technologies). Microarray experiments were performed by the Plateforme Biopuces of Strasbourg using the GeneChip Mouse Gene 1.0 ST array (Affymetrix; see the Supplemental Experimental Procedures). Differentially expressed genes were determined using a stringent min/max procedure (minimum expression among all replicates selected/maximum expression among all other replicates) with a minimal fold change cutoff of two. Gene fold change was given as the mean value of triplicates for subsets displaying the highest and the lowest gene expression. Hierarchical clustering with average linkage was performed with the Gene-E software. String 9.1 software was used to display functional association networks. Microsoft Excel was used to generate heatmaps. Data from the ImmGen compendium of mouse DC subsets were retrieved from NCBI GEO dataset GSE15907 (Heng et al., 2008) and normalized with our own data by Robust Multi-chip Analysis.

Immunofluorescence Staining and Confocal Microscopy
PPs of mice fed or not with 0.2 μ Fluorebrite Yellow Green Microspheres (Polysciences) for 24 hr were fixed with Antigenfix (Diapath) for 1 hr, washed, and processed as previously described (Lelouard et al., 2012). Slides were observed with a Zeiss LSM 780 confocal microscope. Series of z sections were taken for each field to control that microspheres were inside cells. Images were analyzed using Adobe Photoshop CS6 and Imaris 6.1.

Stimulation of PP MPS Subsets and Priming of Th Cells In Vitro
Sorted PP MPS subsets (5 × 10³) were cultured in RPMI-1640 supplemented with 10% fetal calf serum (FCS), 1% GM-CSF, 10% M-CSF, 1% penicillin/streptomycin, 10 mM HEPES, 1 mM sodium pyruvate, 1 mM glutamine, 1 mM non-essential amino-acids, and 50 μM 2-ME with or without R848 (1 μg/ml). After 24 hr, MHCII, CD40, CD80, and CD86 surface expressions were determined by flow cytometry. The concentrations of IL-6, TNF, IL-10, and IFNγ secreted in the culture supernatants were determined using the mouse CBA inflammation kit (BD Biosciences), according to the manufacturer's instructions. OT-II T cells were isolated from lymph nodes of OT-II rag1⁻/⁻ mice (Barnden et al., 1998) using a CD4⁺ T cell-negative isolation kit (Miltenyi). Purified OT-II T cells were incubated with 1 μM CellTrace Violet (CTV; Life Technologies) for 12 min at 37°C. CTV-labeled OT-II T cells (3.5 × 10⁴) were cultured together with sorted PP MPS subsets (3.5 × 10³), pulsed for 2 hr at 37°C with 200 μg/ml endotoxin-free OVA (Hyglos), with or without R848 (1 μg/ml). After 5 days of co-culture, Th cells were restimulated for 4 hr with 10 ng/ml PMA and 1 μg/ml ionomycin in the presence of 10 μg/ml Brefeldin A. Proliferation was measured as a loss of CTV staining. IFNγ production profile of OT-II T cells was determined by intracellular staining. The concentrations of TNF, IFNγ, IL-2, IL-4, IL-6, IL-10, and IL-17 secreted in the supernatants were determined using the mouse CBA Th1/Th2/Th17 cytokine kit (BD Biosciences), according to the manufacturer's instructions.

(D) (Left) 3D reconstruction shows LysoMacs (CD11c in green, lysozyme in red) and LysoDCs (MHCII in green, lysozyme in red) pulsed with OVA and co-cultured with CTV-labeled naive OT-II T cells (cyan) with or without R848 for 16 hr. Note the different steps of degradation of the T cells internalized by a LysoMac. Grid space, 5 μm. (Right) Number of T cells interacting with a single LysoDC with or without R848 stimulation is shown (***p < 0.001, Student's t test; pooled data from three independent experiments). Results of (B and C) are mean ± SD of three independent experiments with 5 × 10³ sorted cells/culture well. See also Figure S5 and Movies S1, S2, S3, S4, and S5.
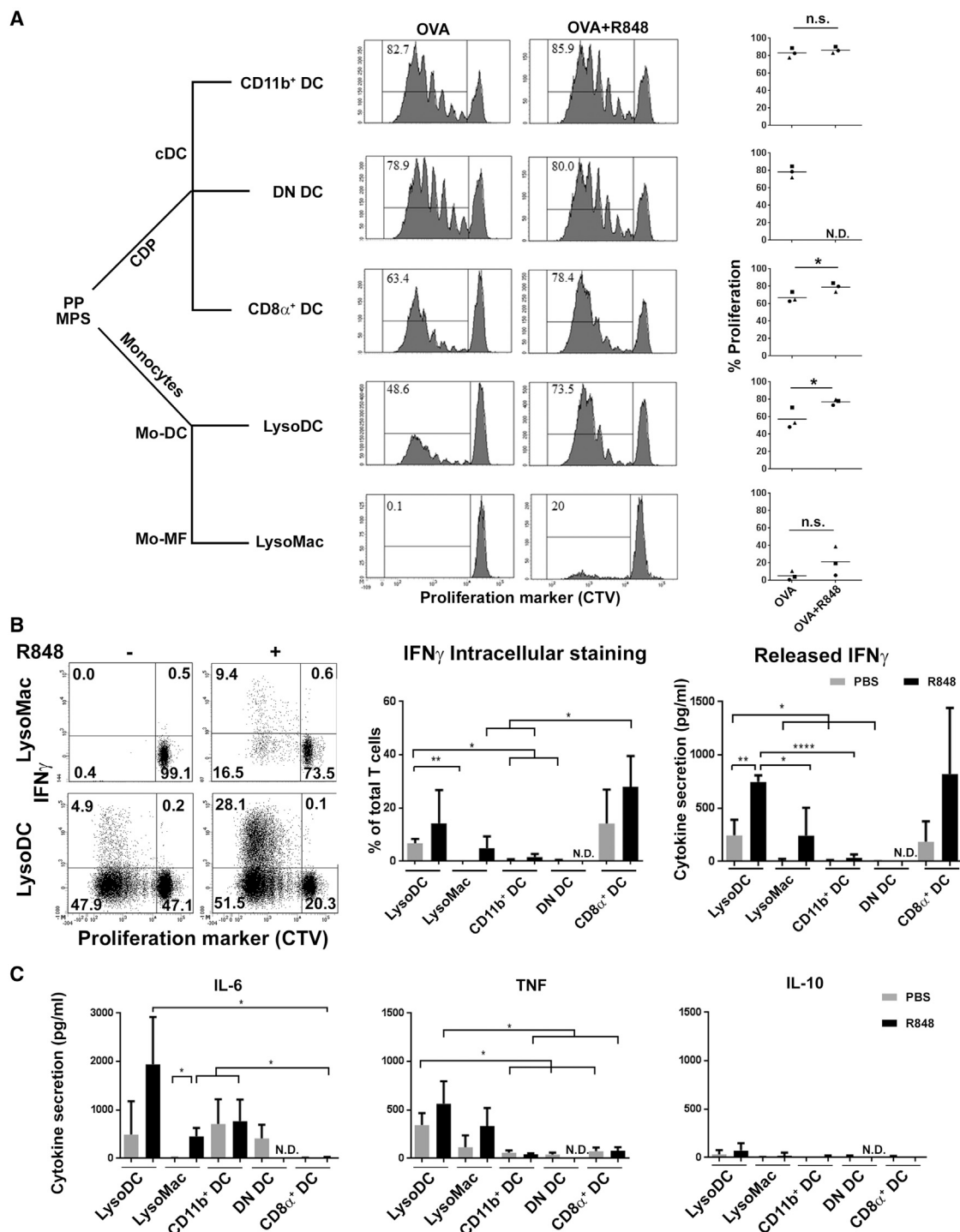
Figure 7. Priming and Polarization of PP DC-Primed Helper T Cells

(A) Proliferation of OT-II T cells (3.5 × 10⁴cells/condition) co-cultured for 5 days with the different PP phagocyte subsets (3.5 × 10³cells/condition) pulsed with OVA and stimulated or not with R848. A representative histogram is shown for each subset as well as a summary of three independent experiments.

(B) (Left) IFNγ intracellular staining of OT-II T cells co-cultured for 5 days with the different PP phagocyte subsets pulsed with OVA and stimulated or not with R848 is shown. (Middle) Percentage of IFNγ-producing cells among total Th cells is shown. (Right) IFNγ secretion in the OT-II T cell co-culture supernatants was determined by cytometric bead array.

(C) IL-6, IL-10, and TNF secretions in the OT-II T cell co-culture supernatants were determined by cytometric bead array. Results of (B and C) are mean ± SD. Data are from three independent experiments with pooled cells from 42 mice per experiment (n.s., non-significant; *p < 0.05, **p < 0.01, ****p < 0.0001, Student's t test).

Statistical Analysis

Results shown as mean ± SD were compared with GraphPad Prism 6 software using Student's t test or one-way ANOVA followed by Bonferroni's multiple comparison test.

ACCESSION NUMBERS

The microarray data reported in this paper have been deposited to the NCBI GEO and are available under accession number GSE65514.

SUPPLEMENTAL INFORMATION

Supplemental Information includes Supplemental Experimental Procedures, six figures, one table, and five movies and can be found with this article online at http://dx.doi.org/10.1016/j.celrep.2015.03.067.

AUTHOR CONTRIBUTIONS

J.B. and H.L. designed and performed the study and analyzed and interpreted the data. H.L. wrote the manuscript. J.-P.G. contributed to the design of the study and revised the manuscript. S.H. contributed to the design and the analysis of the study. C.D.S. and J.B. performed the T cell proliferation and polarization assays. C.D.S. performed the antigen uptake assays. S.H. and S.T. contributed to the parabiosis and chimeric mice experiments. L.C. performed cryostat sectioning. F.M.-S., H.L., and J.B. analyzed the microarray data.

REFERENCES

Albacker, L.A., Karisola, P., Chang, Y.J., Umetsu, S.E., Zhou, M., Akbari, O., Kobayashi, N., Baumgarth, N., Freeman, G.J., Umetsu, D.T., and DeKruyff, R.H. (2010). TIM-4, a receptor for phosphatidylserine, controls adaptive immunity by regulating the removal of antigen-specific T cells. J. Immunol. 185, 6839–6849.

Albacker, L.A., Yu, S., Bedoret, D., Lee, W.L., Umetsu, S.E., Monahan, S., Freeman, G.J., Umetsu, D.T., and DeKruyff, R.H. (2013). TIM-4, expressed by medullary macrophages, regulates respiratory tolerance by mediating phagocytosis of antigen-specific T cells. Mucosal Immunol. 6, 580–590.

Aoshi, T., Koyama, S., Kobiyama, K., Akira, S., and Ishii, K.J. (2011). Innate and adaptive immune responses to viral infection and vaccination. Curr Opin Virol 1, 226–232.

Barnden, M.J., Allison, J., Heath, W.R., and Carbone, F.R. (1998). Defective TCR expression in transgenic mice constructed using cDNA-based alpha- and beta-chain genes under the control of heterologous regulatory elements. Immunol. Cell Biol. 76, 34–40.

Bego, M.G., Mercier, J., and Cohen, E.A. (2012). Virus-activated interferon regulatory factor 7 upregulates expression of the interferon-regulated BST2 gene independently of interferon signaling. J. Virol. 86, 3513–3527.

Blasius, A.L., Giurisato, E., Cella, M., Schreiber, R.D., Shaw, A.S., and Colonna, M. (2006). Bone marrow stromal cell antigen 2 is a specific marker of type I IFN-producing cells in the naive mouse, but a promiscuous cell surface antigen following IFN stimulation. J. Immunol. 177, 3260–3265.

Bogunovic, M., Ginhoux, F., Helft, J., Shang, L., Hashimoto, D., Greter, M., Liu, K., Jakubzick, C., Ingersoll, M.A., Leboeuf, M., et al. (2009). Origin of the lamina propria dendritic cell network. Immunity 31, 513–525.

Boring, L., Gosling, J., Chensue, S.W., Kunkel, S.L., Farese, R.V., Jr., Broxmeyer, H.E., and Charo, I.F. (1997). Impaired monocyte migration and reduced type 1 (Th1) cytokine responses in C-C chemokine receptor 2 knockout mice. J. Clin. Invest. 100, 2552–2561.

Cheong, C., Matos, I., Choi, J.H., Dandamudi, D.B., Shrestha, E., Longhi, M.P., Jeffrey, K.L., Anthony, R.M., Kluger, C., Nchinda, G., et al. (2010). Microbial stimulation fully differentiates monocytes to DC-SIGN/CD209(+) dendritic cells for immune T cell areas. Cell 143, 416–429.

Contractor, N., Louten, J., Kim, L., Biron, C.A., and Kelsall, B.L. (2007). Cutting edge: Peyer's patch plasmacytoid dendritic cells (pDCs) produce low levels of type I interferons: possible role for IL-10, TGFbeta, and prostaglandin E2 in conditioning a unique mucosal pDC phenotype. J. Immunol. 179, 2690–2694.

Dudziak, D., Kamphorst, A.O., Heidkamp, G.F., Buchholz, V.R., Trumpfheller, C., Yamazaki, S., Cheong, C., Liu, K., Lee, H.W., Park, C.G., et al. (2007). Differential antigen processing by dendritic cell subsets in vivo. Science 315, 107–111.

Gautier, E.L., Shay, T., Miller, J., Greter, M., Jakubzick, C., Ivanov, S., Helft, J., Chow, A., Elpek, K.G., Gordonov, S., et al.; Immunological Genome Consortium (2012). Gene-expression profiles and transcriptional regulatory pathways that underlie the identity and diversity of mouse tissue macrophages. Nat. Immunol. 13, 1118–1128.

Geissmann, F., Manz, M.G., Jung, S., Sieweke, M.H., Merad, M., and Ley, K. (2010). Development of monocytes, macrophages, and dendritic cells. Science 327, 656–661.

Ginhoux, F., Liu, K., Helft, J., Bogunovic, M., Greter, M., Hashimoto, D., Price, J., Yin, N., Bromberg, J., Lira, S.A., et al. (2009). The origin and development of nonlymphoid tissue CD103+ DCs. J. Exp. Med. 206, 3115–3130.

Hashimoto, D., Miller, J., and Merad, M. (2011). Dendritic cell and macrophage heterogeneity in vivo. Immunity 35, 323–335.

Hashimoto, D., Chow, A., Noizat, C., Teo, P., Beasley, M.B., Leboeuf, M., Becker, C.D., See, P., Price, J., Lucas, D., et al. (2013). Tissue-resident macrophages self-maintain locally throughout adult life with minimal contribution from circulating monocytes. Immunity 38, 792–804.

Heng, T.S., and Painter, M.W.; Immunological Genome Project Consortium (2008). The Immunological Genome Project: networks of gene expression in immune cells. Nat. Immunol. 9, 1091–1094.

Hildner, K., Edelson, B.T., Purtha, W.E., Diamond, M., Matsushita, H., Kohyama, M., Calderon, B., Schraml, B.U., Unanue, E.R., Diamond, M.S., et al. (2008). Batf3 deficiency reveals a critical role for CD8alpha+ dendritic cells in cytotoxic T cell immunity. Science 322, 1097–1100.

Honda, K., Yanai, H., Negishi, H., Asagiri, M., Sato, M., Mizutani, T., Shimada, N., Ohba, Y., Takaoka, A., Yoshida, N., and Taniguchi, T. (2005). IRF-7 is the master regulator of type-I interferon-dependent immune responses. Nature 434, 772–777.

Hood, M.I., and Skaar, E.P. (2012). Nutritional immunity: transition metals at the pathogen-host interface. Nat. Rev. Microbiol. 10, 525–537.

Iwasaki, A., and Kelsall, B.L. (2001). Unique functions of CD11b+, CD8 alpha+, and double-negative Peyer's patch dendritic cells. J. Immunol. 166, 4884–4890.

Jakubzick, C., Gautier, E.L., Gibbings, S.L., Sojka, D.K., Schlitzer, A., Johnson, T.E., Ivanov, S., Duan, Q., Bala, S., Condon, T., et al. (2013). Minimal differentiation of classical monocytes as they survey steady-state tissues and transport antigen to lymph nodes. Immunity 39, 599–610.

Jung, S., Aliberti, J., Graemmel, P., Sunshine, M.J., Kreutzberg, G.W., Sher, A., and Littman, D.R. (2000). Analysis of fractalkine receptor CX(3)CR1 function by

targeted deletion and green fluorescent protein reporter gene insertion. Mol. Cell. Biol. 20, 4106–4114.

Lelouard, H., Henri, S., De Bovis, B., Mugnier, B., Chollat-Namy, A., Malissen, B., Méresse, S., and Gorvel, J.P. (2010). Pathogenic bacteria and dead cells are internalized by a unique subset of Peyer's patch dendritic cells that express lysozyme. Gastroenterology 138, 173–184, e1–e3.

Lelouard, H., Fallet, M., de Bovis, B., Méresse, S., and Gorvel, J.P. (2012). Peyer's patch dendritic cells sample antigens by extending dendrites through M cell-specific transcellular pores. Gastroenterology 142, 592–601, e3.

Macpherson, A.J., Geuking, M.B., Slack, E., Hapfelmeier, S., and McCoy, K.D. (2012). The habitat, double life, citizenship, and forgetfulness of IgA. Immunol. Rev. 245, 132–146.

Miller, J.C., Brown, B.D., Shay, T., Gautier, E.L., Jojic, V., Cohain, A., Pandey, G., Leboeuf, M., Elpek, K.G., Helft, J., et al.; Immunological Genome Consortium (2012). Deciphering the transcriptional network of the dendritic cell lineage. Nat. Immunol. 13, 888–899.

Miyanishi, M., Tada, K., Koike, M., Uchiyama, Y., Kitamura, T., and Nagata, S. (2007). Identification of Tim4 as a phosphatidylserine receptor. Nature 450, 435–439.

Mora, J.R., Iwata, M., Eksteen, B., Song, S.Y., Junt, T., Senman, B., Otipoby, K.L., Yokota, A., Takeuchi, H., Ricciardi-Castagnoli, P., et al. (2006). Generation of gut-homing IgA-secreting B cells by intestinal dendritic cells. Science 314, 1157–1160.

Nussenzweig, M.C., Steinman, R.M., Witmer, M.D., and Gutchinov, B. (1982). A monoclonal antibody specific for mouse dendritic cells. Proc. Natl. Acad. Sci. USA 79, 161–165.

Owen, R.L., and Jones, A.L. (1974). Epithelial cell specialization within human Peyer's patches: an ultrastructural study of intestinal lymphoid follicles. Gastroenterology 66, 189–203.

Ramsay, A.J., Husband, A.J., Ramshaw, I.A., Bao, S., Matthaei, K.I., Koehler, G., and Kopf, M. (1994). The role of interleukin-6 in mucosal IgA antibody responses in vivo. Science 264, 561–563.

Rubic, T., Lametschwandtner, G., Jost, S., Hinteregger, S., Kund, J., Carbal- lido-Perrig, N., Schwärzler, C., Junt, T., Voshol, H., Meingassner, J.G., et al. (2008). Triggering the succinate receptor GPR91 on dendritic cells enhances immunity. Nat. Immunol. 9, 1261–1269.

Sadler, A.J., and Williams, B.R. (2008). Interferon-inducible antiviral effectors. Nat. Rev. Immunol. 8, 559–568.

Salazar-Gonzalez, R.M., Niess, J.H., Zammit, D.J., Ravindran, R., Srinivasan, A., Maxwell, J.R., Stoklasek, T., Yadav, R., Williams, I.R., Gu, X., et al. (2006). CCR6-mediated dendritic cell activation of pathogen-specific T cells in Peyer's patches. Immunity 24, 623–632.

Sancho, D., and Reis e Sousa, C. (2012). Signaling by myeloid C-type lectin receptors in immunity and homeostasis. Annu. Rev. Immunol. 30, 491–529.

Sato, A., Hashiguchi, M., Toda, E., Iwasaki, A., Hachimura, S., and Kaminogawa, S. (2003). CD11b+ Peyer's patch dendritic cells secrete IL-6 and induce IgA secretion from naive B cells. J. Immunol. 171, 3684–3690.

Satpathy, A.T., Wu, X., Albring, J.C., and Murphy, K.M. (2012). Re(de)fining the dendritic cell lineage. Nat. Immunol. 13, 1145–1154.

Schoggins, J.W., and Rice, C.M. (2011). Interferon-stimulated genes and their antiviral effector functions. Curr Opin Virol 1, 519–525.

Schulz, O., and Pabst, O. (2013). Antigen sampling in the small intestine. Trends Immunol. 34, 155–161.

Schulz, C., Gomez Perdiguero, E., Chorro, L., Szabo-Rogers, H., Cagnard, N., Kierdorf, K., Prinz, M., Wu, B., Jacobsen, S.E., Pollard, J.W., et al. (2012). A lineage of myeloid cells independent of Myb and hematopoietic stem cells. Science 336, 86–90.

Serbina, N.V., and Pamer, E.G. (2006). Monocyte emigration from bone marrow during bacterial infection requires signals mediated by chemokine receptor CCR2. Nat. Immunol. 7, 311–317.

Serbina, N.V., Salazar-Mather, T.P., Biron, C.A., Kuziel, W.A., and Pamer, E.G. (2003). TNF/iNOS-producing dendritic cells mediate innate immune defense against bacterial infection. Immunity 19, 59–70.

Siddiqui, K.R., Laffont, S., and Powrie, F. (2010). E-cadherin marks a subset of inflammatory dendritic cells that promote T cell-mediated colitis. Immunity 32, 557–567.

Tamoutounour, S., Henri, S., Lelouard, H., de Bovis, B., de Haar, C., van der Woude, C.J., Woltman, A.M., Reyal, Y., Bonnet, D., Sichien, D., et al. (2012). CD64 distinguishes macrophages from dendritic cells in the gut and reveals the Th1-inducing role of mesenteric lymph node macrophages during colitis. Eur. J. Immunol. 42, 3150–3166.

Tamoutounour, S., Guilliams, M., Montanana Sanchis, F., Liu, H., Terhorst, D., Malosse, C., Pollet, E., Ardouin, L., Luche, H., Sanchez, C., et al. (2013). Origins and functional specialization of macrophages and of conventional and monocyte-derived dendritic cells in mouse skin. Immunity 39, 925–938.

Tenoever, B.R., Ng, S.L., Chua, M.A., McWhirter, S.M., García-Sastre, A., and Maniatis, T. (2007). Multiple functions of the IKK-related kinase IKKepsilon in interferon-mediated antiviral immunity. Science 315, 1274–1278.

Varol, C., Vallon-Eberhard, A., Elinav, E., Aychek, T., Shapira, Y., Luche, H., Fehling, H.J., Hardt, W.D., Shakhar, G., and Jung, S. (2009). Intestinal lamina propria dendritic cell subsets have different origin and functions. Immunity 31, 502–512.

Waskow, C., Liu, K., Darrasse-Jèze, G., Guermonprez, P., Ginhoux, F., Merad, M., Shengelia, T., Yao, K., and Nussenzweig, M. (2008). The receptor tyrosine kinase Flt3 is required for dendritic cell development in peripheral lymphoid tissues. Nat. Immunol. 9, 676–683.

Yona, S., Kim, K.W., Wolf, Y., Mildner, A., Varol, D., Breker, M., Strauss-Ayali, D., Viukov, S., Guilliams, M., Misharin, A., et al. (2013). Fate mapping reveals origins and dynamics of monocytes and tissue macrophages under homeostasis. Immunity 38, 79–91.

Zhao, X., Sato, A., Dela Cruz, C.S., Linehan, M., Luegering, A., Kucharzik, T., Shirakawa, A.K., Marquez, G., Farber, J.M., Williams, I., and Iwasaki, A. (2003). CCL9 is secreted by the follicle-associated epithelium and recruits dome region Peyer's patch CD11b+ dendritic cells. J. Immunol. 171, 2797–2803.